

Binary accretion rates: dependence on temperature and mass-ratio

M.D. Young¹, and C.J. Clarke¹

¹*Institute of Astronomy, University of Cambridge, Madingley Road, Cambridge, CB3 0HA, United Kingdom*

Written May 21st 2015

ABSTRACT

We perform a series of 2D smoothed particle hydrodynamics (SPH) simulations of gas accretion onto binaries via a circumbinary disc, for a range of gas temperatures and binary mass ratios (q). We show that increasing the gas temperature increases the accretion rate onto the primary for all values of the binary mass ratio: for example, for $q = 0.1$ and a fixed binary separation, an increase of normalised sound speed by a factor of 5 (from our “cold” to “hot” simulations) changes the fraction of the accreted gas that flows on to the primary from 10% to $\sim 40\%$. We present a simple parametrisation for the average accretion rate of each binary component accurate to within a few percent and argue that this parameterisation (rather than those in the literature based on warmer simulations) is relevant to supermassive black hole accretion and all but the widest stellar binaries. We present trajectories for the growth of q during circumbinary disc accretion and argue that the period distribution of stellar “twin” binaries is strong evidence for the importance of circumbinary accretion. We also show that our parametrisation of binary accretion increases the minimum mass ratio needed for spin alignment of supermassive black holes to $q \sim 0.4$, with potentially important implications for the magnitude of velocity kicks acquired during black hole mergers.

1 INTRODUCTION

Understanding the accretion of material onto binaries is important for many astrophysical problems. Super massive black hole binaries are thought to occur frequently as a result of large galactic mergers. However, observationally detecting black hole binaries remains a challenge (Artymowicz & Lubow 1996; Dotti et al. 2012; Schnittman 2013; Bogdanović 2015). As such, understanding the electromagnetic signatures of gas flows onto binaries is important for improving detection. The relative accretion rate of gas by the two binary components is also important in setting the alignment of black hole spins (Bogdanović et al. 2007; Lodato & Gerosa 2013; Gerosa et al. 2015). The alignment of black hole spins sets the recoil velocity of the post-merger black hole and can influence the host galaxy through feedback processes (Blecha & Loeb 2008). Each black hole’s spin is aligned with its disc by the Bardeen-Petterson effect (Bardeen & Petterson 1975), on a time scale which depends upon the accretion rate through the disc (Gerosa et al. 2015). As such, understanding the relative strength of primary (\dot{M}_1) and secondary (\dot{M}_2) accretion is vital for determining the likelihood of spin alignment.

The distribution of stellar mass within binaries is also sensitive to the details of binary accretion. Given that a large fraction of stars are in binaries, this problem is of great significance (Close et al. 2003; Basri & Reiners 2006; Fischer

& Marcy 1992; Duquennoy & Mayor 1991; Preibisch et al. 1999; Mason et al. 1998). It is well known that the initial mass of a protobinary is only a fraction of the mass of the parent cloud (except for the widest binaries) (Boss 1986; Bonnell & Bate 1994). As most of the mass not in the initial protobinary is of greater specific angular momentum, the protobinary can only continue to grow by accreting material through a circumbinary disc. The ultimate mass ratio of the binary ($q = M_2/M_1$, where subscripts 1 and 2 refer to the primary and secondary, respectively) is set by the accretion rates onto the primary (\dot{M}_1) and secondary (\dot{M}_2) through the circumbinary disc.

It is possible that the circumbinary disc that feeds material onto the binaries may be misaligned with the binary orbit. Accretion via a misaligned circumbinary disc does not change the component of the binary that accretes the most material (Nixon et al. 2011, 2013; Dunhill et al. 2014), although the accretion rate is potentially higher for a misaligned circumbinary disc (Nixon et al. 2013).

Cluster level simulations have been used to predict properties of binaries (Goodwin et al. 2004; Offner et al. 2009; Bate 2009; Delgado-Donate & Clarke 2008). They find mass distributions peaked towards high values of q , implying preferential accretion onto the secondary. Dedicated studies of isolated binaries, which allow for much greater resolution, have also been performed using both smoothed particle hy-

drodynamics (SPH) in 3D (Bate & Bonnell 1997; Dotti et al. 2010) and 2D (Young et al. 2015), and using grid codes in 2D (Hanawa et al. 2010; de Val-Borro et al. 2011; Farris et al. 2014). The overwhelming majority of these studies find a strong tendency for the majority of the mass to flow onto the secondary. This is because material flowing from the circumbinary disc encounters the secondary first, since its orbit is further from the centre of mass of the system. Indeed, the same preference for accretion onto the secondary can be found in simulations of ballistic (non-collisional) material with specific angular momentum greater than the binary (Bate 1997).

However, simulations have also shown that gas temperature can moderate this preference for accretion onto the secondary (Dotti et al. 2010; Young et al. 2015). This is because at higher temperatures, material travels from the circumbinary disc onto the binary along a wider range of trajectories, allowing some of it to orbit the edge of the secondary's Roche lobe and accrete onto the primary (Young et al. 2015). Understanding the dependence of relative accretion rate on both gas temperature and binary mass ratio is vital for providing accurate predictions of black hole spin alignment and the distribution of q in stellar clusters. Understanding the temperature dependence of accretion rates is particularly important for black hole applications, where the ratio of sound speed to binary orbital speed is too low to be modeled by current simulations (Gerosa et al. 2015).

In this paper we present a series of SPH calculations of the accretion of gas onto binaries at a range of gas temperatures and mass ratio. We use our simulations to propose a simple parametrisation of the relative accretion rate of binaries, as a function of both gas temperature and mass ratio. In Section 2 we describe the details of our model and the computational set up. In Section 3 we present the results of our simulations. In Section 4 we discuss the interpretation of our results, their implications. Finally we provide some concluding remarks in Section 5.

2 MODEL DETAILS

We model a binary with mass ratio $q = M_2/M_1$, separation a , total mass $M = M_1 + M_2$ on a anti-clockwise circular orbit. All simulations are performed in 2D using a modified version of the SPH code GADGET2 (Springel 2005). We choose to use 2D rather than 3D for comparison to earlier work (Young et al. 2015) and to reduce computational costs (for N particles, resolution scales as $N^{-1/2}$ in 2D and $N^{-1/3}$ in 3D).

Physically, accretion onto a binary is mediated by a circumbinary accretion disc. As viscosity in this disc causes it to spread inwards, material flows from the edge of the circumbinary disc onto the binary. Self consistent modelling of this viscous spreading, which is primarily driven by an effective viscosity resulting from turbulent processes (Pringle 1981; Shakura & Sunyaev 1973), is computationally challenging for binary accretion modeling and has not to date been extended to studying accretion onto the individual binary components (Shi et al. 2012). Furthermore, the details of the accretion in the circumbinary disc are unlikely to affect the steady-state accretion rate of the binary. Given this, we choose to follow Bate & Bonnell (1997) & Young et al.

(2015) and inject material at a fixed boundary far from the binary, $R = R_{inf}a$, with fixed specific angular momentum, $j = j_{inf}\sqrt{GMa}$. The initial radial velocity of material at the outer edge is set such that the material is initially marginally gravitationally bound. This allows us to provide a continuous supply of material to the binary, without the computational expense of simulating a large circumbinary disc.

The mass of the gas is taken to be negligible compared to the binary and so the self-gravity of the gas is ignored. For the same reason, the binary masses and orbits remain fixed throughout our simulations. Any particle which is within $R = R_{acc}a$ of a binary particle is removed from the simulation and the number of removed particles per binary particle is recorded (we set $R_{acc} = .02$ in all our simulation). The gas temperature is modeled using an isothermal equation of state, which is parametrised in terms of c :

$$c = c_s / \sqrt{\frac{GM}{a}} \quad (1)$$

c is then the sound speed normalised to the orbital speed of the binary (it is also H/R of the circumbinary disc at a radius of a).

For all simulations performed here we set $j_{inf} = 1.2$ and $R_{inf} = 20$ which ensures a constant supply of material onto the binary with specific angular momentum similar to what would be expected for material at the inner edge of a circumbinary disc (Bate & Bonnell 1997; Bate 2000). Lower values of j_{inf} would be unrealistic for accretion via a disc, while higher values of j_{inf} would cause a disc to form at a radii where material cannot flow onto the binary until viscous spreading moved the boundary inwards. We inject particles at the boundary at a rate of $\dot{N} = 500$ per dynamical time, which ensures the edge of the circumstellar discs are well resolved (Young et al. 2015). As the temperature of the gas has been shown to affect the relative accretion rate of binary components, we explore values in the range $c = 0.05 - 0.25$. As lower values of c produce thinner discs which require more resolution elements to resolve, we were unable to probe values of $c < 0.05$. We run simulations with $0.1 < q < 1.0$ to explore the effect of q on relative accretion rates. Smaller values of $q < 0.1$ were deliberately excluded as they are more computationally demanding and the nature of the accretion flow has been shown to change qualitatively in this range. That is, for $q < 0.1$, the accretion transitions from gas flowing onto a binary in a low gas density cavity, to gas flowing through a large circumprimary disc, with a large embedded body clearing a gap (D'Orazio et al. 2013). Each simulation was run for at least 500 binary dynamical times, by which time they have settled into a steady-state (Young et al. 2015).

All analysis was performed in a frame corotating with the binary, translated so that the primary is at the origin and the secondary is at $(x,y)=(-1,0)$. In this reference frame it is possible to define a modified potential, commonly called the ‘‘Roche potential’’, as:

$$\Phi = -\frac{GM_1}{|\mathbf{r} - \mathbf{r}_1|} - \frac{GM_2}{|\mathbf{r} - \mathbf{r}_2|} - \frac{1}{2}(\mathbf{\Omega} \times \mathbf{r})^2 \quad (2)$$

where $\mathbf{\Omega}$ is the angular momentum vector of the binary, \mathbf{r} is the position vector and subscripts 1 and 2 refer to the primary and secondary respectively. Surfaces of equipotential of Φ and Lagrange points (points of zero gradient) are shown in Figure 1.

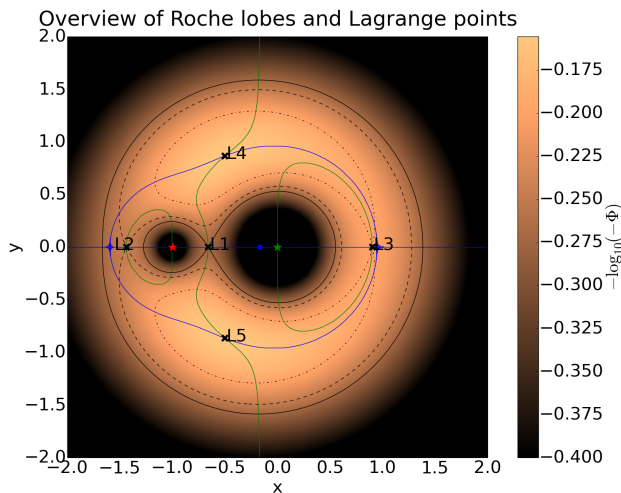


Figure 1. Equipotential surfaces of Φ , the modified potential (gravitational potential plus term to include centrifugal force of non-inertial frame) for the values of Φ obtained at the three Lagrange points L1, L2 and L3. The colour map shows Φ elsewhere. The stars are marked in red (secondary) and green (primary) and the centre of mass of the system is marked in blue. The green and blue lines are the locations where the x and y components of the force resulting from this potential (i.e., $-\nabla\Phi$) are zero.

ID	q	c	t_{end}
1	0.1	0.05	720
2	0.2	0.05	500
3	0.3	0.05	640
4	0.4	0.05	630
5	0.5	0.05	690
6	0.6	0.05	720
7	0.7	0.05	730
8	0.8	0.05	840
9	0.9	0.05	800
10	0.1	0.25	2000
11	0.2	0.25	2000
12	0.3	0.25	2000
13	0.4	0.25	2000
14	0.5	0.25	2000
15	0.6	0.25	2000
16	0.7	0.25	2000
17	0.8	0.25	2000
18	0.9	0.25	2000
19	0.1	0.10	542
20	0.1	0.15	521
21	0.1	0.20	515

Table 1. Parameters used for simulations in this paper. For each simulation particles were injected at a rate of roughly $\dot{N} \approx 500$ per dynamical time ($\sqrt{a^3/GM}$), the accretion radius was set to $0.02a$, particles were injected from $20a$ with specific angular momentum $1.2\sqrt{GMa}$.

Table 1 lists the parameters used for all simulations in this paper. Details of the exact version of the SPH code used along with initial conditions and parameter files can be found in Section 6.

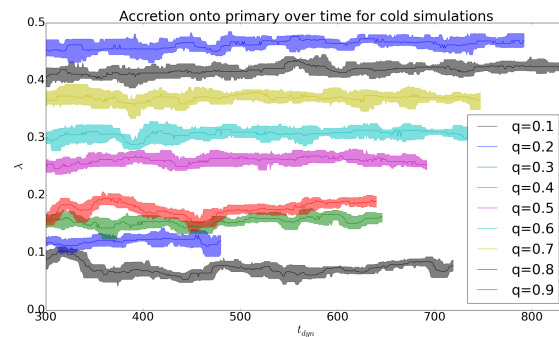


Figure 2. Steady-state values of $\lambda = \dot{M}_1/\dot{M}$ for simulations with cold gas ($c = 0.05$), for a range of values of q . The central line shows a moving average over 3 binary orbits of λ while the shaded region shows the one standard deviation range on λ within this range. The first 200 binary dynamical times are omitted to ensure that only steady-state accretion is shown.

3 RESULTS

All our simulations undergo a transient settling phase, which is dependent on the details of the initial conditions, before settling into a steady-state after ~ 30 binary orbits. To exclude the physically uninteresting effects of this settling phase, we excluded the first 200 dynamical times (where 2π dynamical times is one binary orbit) from all the results that follow.

The evolution of the binary mass ratio q and the relative strength of primary/secondary accretion flows can be characterised using the parameter,

$$\Gamma = \frac{\dot{q}}{q} \frac{\dot{M}}{\dot{M}} = \frac{(1+q)}{q\dot{M}} (\dot{M}_2 - q\dot{M}_1) \quad (3)$$

which is the fractional change in q per fractional change in \dot{M} . This can be re-written as,

$$\Gamma = \frac{(1+q)}{q} (1 - \lambda(1+q)) \quad (4)$$

where $\lambda = \dot{M}_1/\dot{M}$ and $\dot{M} = \dot{M}_1 + \dot{M}_2$. In our simulations we measure \dot{M}_1 and \dot{M}_2 by counting the number of particles accreted onto the primary and the secondary.

The evolution of λ as a function of time and q is shown for simulations with cold gas ($c = 0.05$) in Figure 2. λ is smoothed using a moving average over three binary orbits, which is roughly the orbital period of the edge of the binary cavity.

Figure 3 shows the same information for the hot simulations (where $c = 0.25$). Unlike the cold simulations the accretion rate λ is significantly more variable, making it difficult to discern any trend in the average accretion rate with q .

Figure 4 show the distribution of λ in the steady-state for all simulations. This allows the trends in the average accretion rate with q and c to be more clearly visualised. The cross in each distribution shows an estimate of the average steady-state λ , given by $\int \dot{M}_1 / \int \dot{M}$.

Figure 4 also shows the distribution of steady-state accretion rates for a series of simulations with $q = 0.1$ and gas temperatures intermediate between hot ($c = .25$) and

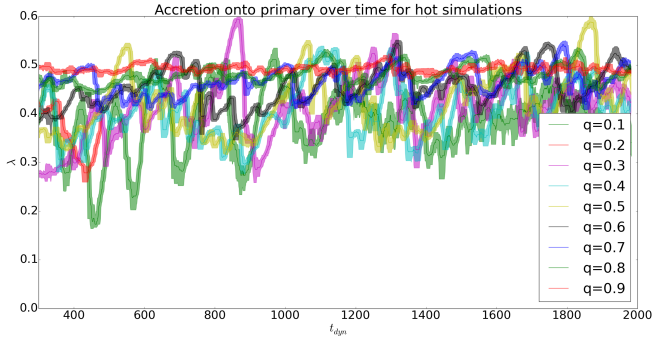


Figure 3. The same as Figure 2 but for simulations with hot gas ($c = 0.25$).

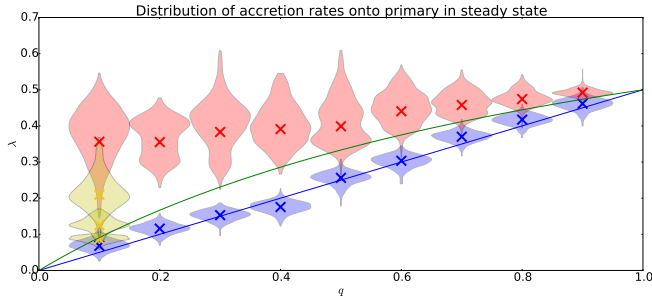


Figure 4. The distribution of steady state λ for all simulations. Each simulation is represented by a violin plot, where more common values of λ correspond to a greater horizontal extent. The crosses show the average steady-state accretion rate across the entire simulation (excluding $t < 200t_{dyn}$), $\int \dot{M}_1 / \int \dot{M}$. Hot simulations are shown in red, cold simulations in blue and intermediate simulations in yellow. The blue line shows the parametrisation $\lambda = q/2$ and the green line shows $\lambda = \frac{q}{q+1}$.

cold ($c = .05$). These additional simulations show how the accretion rate changes with gas temperature in more detail.

4 DISCUSSION

4.1 Variability of λ

All simulations show a significant amount of temporal variability in λ . This variability is driven by fluctuations in the amount of material flowing into the binary cavity, which has been identified in many previous simulation of gas flow onto binaries (D’Orazio et al. 2013; Ochi et al. 2005; Young et al. 2015; Artymowicz & Lubow 1996; MacFadyen & Milosavljević 2008; Shi et al. 2012).

The physical mechanism for the variability in supply of material onto the binary was explained in detail by MacFadyen & Milosavljević (2008) & D’Orazio et al. (2013). They found that the edge of the circumbinary disc was eccentric (i.e., the cavity wall is not circular). Because of this, the amount of material flowing inwards fluctuates on the time scale of, 1) the binary orbit and 2) the precession time scale of the disc edge.

Because changes in the rate of flow onto the binary are

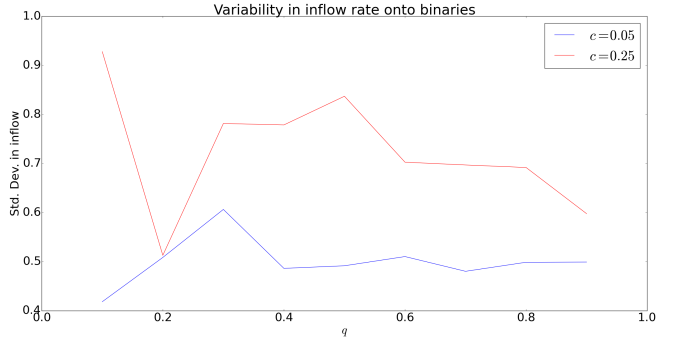


Figure 5. The vertical axis is the standard deviation in the rate of inflow onto either Roche lobe, divided by the particle injection rate at the outer boundary (i.e., the standard deviation of the inflow rate into the cavity). As with all other quantities, the first 200 dynamical times were excluded from the calculation so that only the steady state is probed.

driven by disc eccentricity, the magnitude of the variability (and the importance of the different time scales) varies with q . Generally, a larger q is able to excite a more eccentric cavity edge, which leads to greater variability (see D’Orazio et al. (2013) for details of the physical mechanism). Figure 5 shows the variability in the amount of gas flowing inwards past the Roche equipotential surface passing through the L1 point. Although there is significant variability in the infall rate, the amount of variability does not change systematically with q . This is likely a limitation of our decision to inject material with constant angular momentum $j = 1.2\sqrt{GMa}$, which prevents the disc edge reaching high eccentricities (MacFadyen & Milosavljević (2008); Shi et al. (2012) found $e \sim 0.1 - 0.4$ for $q = 1.0$) by providing a flow of material that will push the disc towards a circular flow beyond the circularisation radius of $R = j_{in,f}^2/a$. On the other hand, a trend towards increased variability at higher gas temperatures can clearly be seen.

Unlike Figure 5, Figure 4 shows a clear trend towards the accretion rate onto either component of the binary becoming *less* variable as q increases. This is because λ (and the accretion onto the secondary, $1 - \lambda$) measures the accretion rate through the inner edge of the discs around each component of the binary. Material flows from the edge of the circumbinary disc onto either the circumprimary or circumsecondary disc. To reach the inner edge and be accreted, it must be “processed” by the circumstellar disc. That is, material that joins the circumprimary disc is only registered at the inner edge once that material has been moved there by the circumprimary disc’s viscosity. For discs with lower viscosity (e.g. colder discs) or with a greater spatial extent (e.g. discs with higher q), variability in the supply of material at the outer edge will be more smeared out by the time the inner edge is reached.

Given this, the variability in Figure 4 is likely driven largely by numerics, with simulations with hotter gas and/or larger discs (i.e. higher q) transmitting more of the variability in supply of material striking the discs around each binary component through to the inner edge where it is accreted. Physically realistic discs, with significantly lower viscosity than the numerical viscosity of our simulations,

greater dynamic range in disc radius and lower gas temperatures, will have much less variability in the accretion rate onto the components of the binary than our simulations. However, the average accretion rate over many binary orbits should be independent of the amount of numerical variability. This can be seen in the simulations of Young et al. (2015), where the magnitude of the variability decreases with resolution but the average accretion rate is unchanged.

4.2 Parametrisation of λ

The most important quantity to understand for our purposes is the steady-state value of λ , which uniquely determines the fractional accretion rate Γ via Equation 4. For the reasons discussed in the previous section, it is the steady state average of λ which is important in determining the physical properties of the binary.

It was recently suggested by Gerosa et al. (2015), that λ can be parametrised as,

$$\lambda = \frac{q}{q+1} \quad (5)$$

based upon the data of Farris et al. (2014), who simulated accretion onto binaries using a grid-based code for a range of values of q and intermediate temperature gas ($c = 0.10$).

The green line in Figure 4 shows this parametrisation. It is clear that this expression is appropriate for binaries accreting gas of intermediate temperature (understandable, given the source data), but provides a poor estimate for the accretion of hot or cold gas.

By symmetry, any parametrisation must have $\lambda = 0.5$ when $q = 1$. Based on the data in Figure 4, we propose the simple parametrisation

$$\lambda = \frac{1}{2} + m(q-1) \quad (6)$$

where m is a function of c and $m \rightarrow 0.5$ as $c \rightarrow 0$. The cold limit, where $\lambda = q/2$, is shown in blue in Figure 4 and is accurate for the cold simulations to within a few percent.

To assess how m in Equation 6 varies with c , we calculated the best fit value of m to the data using least squares minimisation, which we plot in Figure 6. It is clear that an asymptotic limit of $m = 0.5$ is appropriate for the cold limit and that m decreases as a strong power of c . We have avoided giving a functional form for m given that we have relatively few data points in c and the values of m for $c = 0.10, 0.15$ and 0.20 are fit using only one sampling in q .

Moreover, it is the cold limit which is most applicable to the bulk of astrophysical systems. In the case of protobinaries, c is likely to lie in the range $\sim 0.01 - 0.1$ (Young et al. 2015). For black hole binaries, normalised sound speeds as low as .001 are possible (Gerosa et al. 2015). In either case, our results suggest that the binary accretion rate should be well approximated by,

$$\Gamma = \frac{(1-q^2)(2+q)}{2q} \quad (7)$$

As well as being in good agreement with the results of Section 3, this parametrisation is also consistent with the finding of earlier simulations of cold gas accreting onto binaries (Bate & Bonnell 1997; Young et al. 2015).

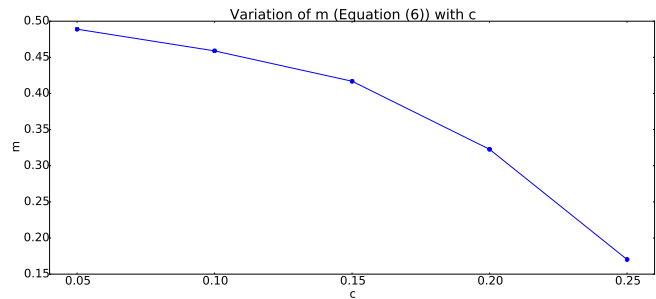


Figure 6. The best fit value of the parameter m in the parametric model for λ given by Equation 6. For each value of c Equation 6 was fit using the average steady state value of λ for each q . Note that the values for $c = 0.10, 0.15$ & 0.20 are fit using just one data point.

4.3 Implications

For all values of parameter space that we explored, we find $\Gamma > 0$, implying that accreting material onto a binary always brings its mass ratio closer to 1. It has been shown that when $q < 0.1$, a region of parameter space we chose not to explore, the physical behaviour of the accretion flow transitions to that of a planet embedded in a disc, causing Γ to fall (D’Orazio et al. 2013; Farris et al. 2014). It is possible that for very small values of q , Γ may become negative, but this would need to be confirmed with specialised simulations.

By integrating Equation 7, we can determine how q evolves as a function of accreted mass. This is shown for both hot and cold simulations (dashed and solid lines, respectively) in Figure 7. Note that this plot is somewhat different from those presented in Bate (2000), in which a protobinary was evolved subject to infall from a variety of parent cores. The resulting evolution in q was then sensitive not only to the density and angular velocity profile of the cores, but also to the assumptions made about protobinary migration. Specifically, \dot{M}_1/\dot{M}_2 depends on the specific angular momentum of the infalling gas *relative to the binary*, which changes as the binary migrates. Here we define the initial binary as corresponding to the point at which it begins to accrete from a circumbinary disc. From this point on, the material accreted onto the binary must always be of similar specific angular momentum to the binary and so q simply evolves along the appropriate path in Figure 7. Figure 7 is therefore readily applicable to either the stellar binary or black hole case.

4.3.1 Application to stellar binaries

Main sequence binary star surveys of solar type stars reveal a remarkable population of “twin-like” binaries ($q > 0.95$; Raghavan et al. (2010))¹. In the light of Figure 7 and given the lack of obvious mechanisms that otherwise produce such

¹ The existence of these “twin-like” binaries is not in doubt, however, there may be some under-representation of the lowest q binaries as their abundance must be corrected in surveys which are incomplete (Goldberg et al. 2003).

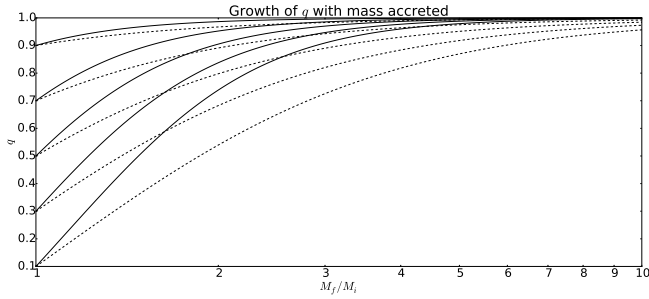


Figure 7. Change in q as a function of accreted mass over initial binary mass, for cold gas with $\lambda = q/2$ (solid line) and hot gas with $\lambda = 0.17q + 0.33$ (dashed line).

strongly correlated masses, it is natural to ascribe these objects to mass equalisation by circumbinary disc accretion. Figure 7 implies that such twin-like systems can be produced from a wide range of initial q values, provided that the binary accretes of order several times its own mass from a circumbinary disc. On the other hand studies of binary migration during circumbinary disc accretion all concur that the (inward) migration time is less than or of the same order as the mass doubling time (MacFadyen & Milosavljević 2008; Shi et al. 2012; Cuadra et al. 2009). This immediately implies that “twin-like” systems have migrated inwards by a large factor. A further corollary is that the parent system (binary plus circumbinary disc) would in the past have contained an angular momentum that is considerably larger than that contained in the present day binary².

The period distribution of “twin-like” binaries amply supports this picture. The angular momentum budget of pre-stellar cores (Goodman et al. 1993) is only sufficient to form binaries out to separations of order 10^3 A.U.³ Given that the angular momentum in the final binary is only a fraction of the angular momentum needed to drive a binary into a twin-like state, it is unsurprising that the maximum separation of twin-like objects is considerably less than this (~ 100 A.U.). On the other hand, low q systems are relatively uncommon at small separations (< 5 A.U.); this again is consistent with a picture in which the bulk of close binaries are driven to small separation by circumbinary accretion (rather than simply arising from cores with exceptionally low specific angular momentum).

Figure 7 also shows that more accreted mass is needed to equalise the mass of binaries when the gas is “hot”. As the normalised sound speed and seed protobinary mass as

a fraction of total core mass both increase with binary separation (Young et al. 2015; Boss 1986; Bate 2000), binaries evolve less far to the right (as less M_f/M_i gas mass is available to be accreted) and along slower tracks (as the gas is “hotter”) in Figure 7. As such, we expect small separation binaries to have q distributions strongly biased towards $q = 1$, while wide binaries should show a much weaker preference for equal mass binaries, again consistent with the picture described above.

4.3.2 Black hole binaries

Gerosa et al. (2015) examined whether circumbinary accretion onto black holes can align their spins with the circumbinary disc on the timescale on which they are driven inwards by circumbinary disc torques. This analysis involved prescriptions for total binary accretion rate, disc mediated migration, accretion induced spin alignment and the relative accretion rates onto the binary components as a function of q . The latter prescription was derived from the simulations of Farris et al. (2014). In conjunction with the other model assumptions it was concluded that whereas the secondary always aligns with the circumbinary disc, the primary remains misaligned for $q < 0.2$. Misaligned spins at the point of binary merger have important consequences for the recoil velocities resulting from the merger event.

If we repeat this analysis but instead use our prescriptions for differential mass acquisition (which are more appropriate for the ‘cold’ conditions expected in the black hole case) we find that it is easier for black hole spins to remain misaligned: for the fiducial model this increases the maximum q value for misalignment from $q = 0.2$ to $q = 0.4$. This is because we find a stronger preference for accretion on to the secondary than in the warmer Farris et al. (2014) simulations; consequently the primary is relatively starved of accretion and can remain misaligned at higher q values. Our result thus strengthens the result of Gerosa et al. (2015), implying a significant population of black holes whose spins are expected to be misaligned at the point of merger.

When black holes with misaligned spins merge, the merger product receives a velocity “kick”, the maximum value of which scales as $\eta = q/(1+q)^2$ (Lousto & Zlochower 2013). For binaries with $q \gtrsim 0.4$ the maximum merger kick velocity may be comparable with the escape velocity of typical elliptical galaxies (Merritt et al. 2004). Moreover, the fact that binaries may enter the gravitational wave inspiral regime with misaligned spins and relatively large q has potential implications for the richness of the gravitational wave signature potentially detectable by e-LISA.

There is however a *caveat* to this. The prescriptions of Gerosa et al. (2015) imply that the binary mass doubling timescale is much greater than its migration timescale and in this limit it is appropriate to consider spin alignment at constant q . However, recent work employing ‘live’ MRI turbulence in the gas flow finds a mass doubling time which is only modestly in excess of the migration time (Shi et al. 2012). If this is correct then migration by a large factor (i.e. the ~ 10 fold shrinkage that is required before migration due to gravitational wave emission becomes effective), also implies a significant change in binary mass (and thus, by Figure 7, the value of q). Indeed we have seen above that in the stellar case there is ample observational evidence for

² The simulations presented here have been artificially set up so that the specific angular momentum of the infalling material only modestly exceeds that of the binary in order to mimic the inner parts of a circumbinary disc in a computationally efficient manner; in reality, however, the inner regions of such a disc are fed by viscous redistribution within a reservoir of material whose mean specific angular momentum far exceeds that of the binary and this becomes increasingly true as the binary migrates inwards.

³ Wider binaries are attributed either to cluster mediated capture (Kouwenhoven et al. 2010; Moeckel & Clarke 2011) or to orbital reconfiguration in multiples producing wide companions on high eccentricity, low angular momentum orbits (Reipurth & Mikkola 2012).

a preference for high q pairs at small separation. It is not clear in the black hole case whether there is a sufficiently large mass reservoir in the circumbinary disc to effect a significant change in q and it is also unclear whether (for a restricted mass reservoir) the relatively strong accretion on to the binary limits how far it will migrate. Pending further theoretical work in this area, we cannot rule out the possibility that even low q pairs might not eventually attain a high enough value of q for the primary to also align with the circumbinary disc.

5 CONCLUSIONS

In this paper we have shown that the mass accretion rates of the primary and secondary components of binaries depend on the gas temperature. We have shown that for all values of q , increasing the gas temperature allows more material to accrete onto the primary component of the binary. The relative accretion by the primary, \dot{M}_1/\dot{M} , is also found to increase at least quadratically with the sound speed of the accreted gas.

Although our simulations show a range of levels of variability of accretion onto the star, we argue that it is only the higher than physical disc viscosity and lower than physical dynamic range in disc radii that allows variability in the mass influx at the Roche lobe to be manifest as variable accretion onto the star. For realistic physical discs any variability in the inflow rate will be smoothed out by the circumpriary/secondary disc and the variability in the accretion rate onto the binary components will be low. As such, it is the average steady-state accretion rate that is the physically relevant quantity in our simulations.

We have proposed a simple parametrisation of the relative accretion rates onto the two components of the binary and shown that it reduces to,

$$\frac{\dot{M}_1}{\dot{M}} = \frac{q}{2} \quad (8)$$

and

$$\frac{\dot{M}_2}{\dot{M}} = \frac{2-q}{2} \quad (9)$$

when the accreted gas is cold.

We argue that the period distribution of “twin-like” stellar binaries provides strong evidence that these objects acquired the bulk of their mass through circumbinary accretion and that they have migrated inwards by a large factor from their initial birthplaces. Applying our parametrisation to super massive black hole binaries with existing models for spin alignment we find that black hole spins’ remain unaligned when q is less than 0.4. However, this value may be decreased if the mass accreted during the black hole merger is sufficient to drive significant evolution in q .

6 MATERIALS & METHODS

In the interests of reproducibility and transparency, all the code needed to reproduce this work has been made freely available online at <https://bitbucket.org/constantAmateur/binaryaccretion>. See the readme file in this repository for further details.

All figures in this paper were generated using the python package MATPLOTLIB (Hunter 2007).

7 ACKNOWLEDGEMENTS

We would like to thank Davide Gerosa, Giuseppe Lodato and Giovanni Rosotti for useful discussions. We thank Giovanni Rosotti for a critical reading and comments on the manuscript. We acknowledge an anonymous referee for their comments which improved the manuscript.

We are indebted to Eduardo Delgado-Donate who was working on this problem at the time of his untimely death in 2007.

This work has been supported by the DISCSIM project, grant agreement 341137 funded by the European Research Council under ERC-2013-ADG. Supercomputer time was provided through DiRAC project grants DP022 & DP047.

This work used the DIRAC Shared Memory Processing system at the University of Cambridge, operated by the COSMOS Project at the Department of Applied Mathematics and Theoretical Physics on behalf of the STFC DiRAC HPC Facility (www.dirac.ac.uk). This equipment was funded by BIS National E-infrastructure capital grant ST/J005673/1, STFC capital grant ST/H008586/1, and STFC DiRAC Operations grant ST/K00333X/1. DiRAC is part of the National E-Infrastructure.

This work used the DiRAC Data Analytic system at the University of Cambridge, operated by the University of Cambridge High Performance Computing Service on behalf of the STFC DiRAC HPC Facility (www.dirac.ac.uk). This equipment was funded by BIS National E-infrastructure capital grant (ST/K001590/1), STFC capital grants ST/H008861/1 and ST/H00887X/1, and STFC DiRAC Operations grant ST/K00333X/1. DiRAC is part of the National E-Infrastructure.

REFERENCES

- Artymowicz P., Lubow S. H., 1996, ApJ, 467, L77
- Bardeen J. M., Petterson J. A., 1975, ApJ, 195, L65
- Basri G., Reiners A., 2006, AJ, 132, 663
- Bate M. R., 1997, MNRAS, 285, 16
- Bate M. R., 2000, MNRAS, 314, 33
- Bate M. R., 2009, MNRAS, 392, 590
- Bate M. R., Bonnell I. A., 1997, MNRAS, 285, 33
- Blecha L., Loeb A., 2008, MNRAS, 390, 1311
- Bogdanović T., 2015, Astrophysics and Space Science Proceedings, 40, 103
- Bogdanović T., Reynolds C. S., Miller M. C., 2007, ApJ, 661, L147
- Bonnell I. A., Bate M. R., 1994, MNRAS, 271, 999
- Boss A. P., 1986, ApJS, 62, 519
- Close L. M., Siegler N., Freed M., Biller B., 2003, ApJ, 587, 407
- Cuadra J., Armitage P. J., Alexander R. D., Begelman M. C., 2009, MNRAS, 393, 1423
- de Val-Borro M., Gahm G. F., Stempels H. C., Pepliński A., 2011, MNRAS, 413, 2679

- Delgado-Donate E. J., Clarke C. J., 2008, in Hubrig S., Petr-Gotzens M., Tokovinin A., eds, *Multiple Stars Across the H-R Diagram The Formation of Multiple Stars*. p. 87
- D’Orazio D. J., Haiman Z., MacFadyen A., 2013, *MNRAS*, 436, 2997
- Dotti M., Sesana A., Decarli R., 2012, *Advances in Astronomy*, 2012, 3
- Dotti M., Volonteri M., Perego A., Colpi M., Ruszkowski M., Haardt F., 2010, *MNRAS*, 402, 682
- Dunhill A. C., Alexander R. D., Nixon C. J., King A. R., 2014, *MNRAS*, 445, 2285
- Duquenois A., Mayor M., 1991, *A&A*, 248, 485
- Farris B. D., Duffell P., MacFadyen A. I., Haiman Z., 2014, *ApJ*, 783, 134
- Fischer D. A., Marcy G. W., 1992, *ApJ*, 396, 178
- Gerosa D., Veronesi B., Lodato G., Rosotti G., 2015, *ArXiv e-prints*
- Goldberg D., Mazeh T., Latham D. W., 2003, *ApJ*, 591, 397
- Goodman A. A., Benson P. J., Fuller G. A., Myers P. C., 1993, *ApJ*, 406, 528
- Goodwin S. P., Whitworth A. P., Ward-Thompson D., 2004, *A&A*, 414, 633
- Hanawa T., Ochi Y., Ando K., 2010, *ApJ*, 708, 485
- Hunter J. D., 2007, *Computing In Science & Engineering*, 9, 90
- Kouwenhoven M. B. N., Goodwin S. P., Parker R. J., Davies M. B., Malmberg D., Kroupa P., 2010, *MNRAS*, 404, 1835
- Lodato G., Gerosa D., 2013, *MNRAS*, 429, L30
- Lousto C. O., Zlochower Y., 2013, *Phys. Rev. D*, 87, 084027
- MacFadyen A. I., Milosavljević M., 2008, *ApJ*, 672, 83
- Mason B. D., Gies D. R., Hartkopf W. I., Bagnuolo Jr. W. G., ten Brummelaar T., McAlister H. A., 1998, *AJ*, 115, 821
- Merritt D., Milosavljević M., Favata M., Hughes S. A., Holz D. E., 2004, *ApJ*, 607, L9
- Moeckel N., Clarke C. J., 2011, *MNRAS*, 415, 1179
- Nixon C., King A., Price D., 2013, *MNRAS*, 434, 1946
- Nixon C. J., King A. R., Pringle J. E., 2011, *MNRAS*, 417, L66
- Ochi Y., Sugimoto K., Hanawa T., 2005, *ApJ*, 623, 922
- Offner S. S. R., Hansen C. E., Krumholz M. R., 2009, *ApJ*, 704, L124
- Preibisch T., Balega Y., Hofmann K.-H., Weigelt G., Zinnecker H., 1999, *New.Astron.*, 4, 531
- Pringle J. E., 1981, *ARA&A*, 19, 137
- Raghavan D., McAlister H. A., Henry T. J., Latham D. W., Marcy G. W., Mason B. D., Gies D. R., White R. J., Ten Brummelaar T. A., 2010, *VizieR Online Data Catalog*, 219, 1
- Reipurth B., Mikkola S., 2012, *Nat*, 492, 221
- Schnittman J. D., 2013, *Classical and Quantum Gravity*, 30, 244007
- Shakura N. I., Sunyaev R. A., 1973, *A&A*, 24, 337
- Shi J.-M., Krolik J. H., Lubow S. H., Hawley J. F., 2012, *ApJ*, 749, 118
- Springel V., 2005, *MNRAS*, 364, 1105
- Young M. D., Baird J. T., Clarke C. J., 2015, *MNRAS*, 447, 2907